Fluidized bed combustion characteristics of high-ash coal char under O2/H2O and O2/CO2/H2O environments

Fuel Processing Technology 284 (2026) 108415

Contents lists available at ScienceDirect

Fuel Processing Technology

journal homepage: www.elsevier.com/locate/fuproc

Research article

Fluidized bed combustion characteristics of high-ash coal char under O_2/H_2O and $O_2/CO_2/H_2O$ environments

Sachin K.S. [a], David Pallarès [b,*], Bo Leckner [b], Pratikash Panda [a,c], R.V. Ravikrishna [a,d]

[a] Interdisciplinary Centre for Energy Research, Indian Institute of Science, Bangalore, 560012, Karnataka, India
[b] Department of Space, Earth and Environment, Chalmers University of Technology, S-41296, Gothenburg, Sweden
[c] Department of Aerospace Engineering, Indian Institute of Science, Bangalore, 560012, Karnataka, India
[d] Department of Mechanical Engineering, Indian Institute of Science, Bangalore, 560012, Karnataka, India

ARTICLE INFO

Keywords:
$O_2/CO_2/H_2O$ combustion
High ash coal
In-situ prepared char
Oxy-steam
Oxy fuel
Particle temperature
UEGO sensor

ABSTRACT

The combustion characteristics of a batch of in-situ prepared high-ash coal char have been investigated under different fluidized bed operating conditions (i.e. O_2 concentration, balance gas, bed temperature, particle size) in an optically accessible fluidized bed. A fast Universal Exhaust Gas Oxygen (UEGO) sensor measured the oxygen partial pressure at the exhaust to determine the reaction rate and burnout time of char particles, which demonstrates a novel application of this type of sensor in high H_2O (wet) environments. A pre-calibrated two-colour pyrometry technique was employed to measure the temperature of char particles. The effect of the oxyfuel atmosphere on the burnout time of char particles was found to be prominent at higher bed temperatures, lower O_2 concentrations, and larger particle sizes. The sensitivity of combustion behaviour to variations in the combustion environment was higher for larger particle size. Results show that the burnout time was the lowest in O_2/H_2O for both 1.2 mm and 3 mm particle sizes. This was attributed to the higher diffusivity of O_2 in H_2O and the H_2O gasification reaction. The addition of H_2O to O_2/CO_2 environment enhanced the diffusivity of O_2, making it comparable to that in N_2. In 10% O_2/45% CO_2/45% H_2O environment, competitive interactions among O_2, CO_2 and H_2O were more pronounced for smaller particles. The reactivity of char in 10% O_2/90% H_2O at higher bed temperatures became comparable to that in 20% O_2/80% N_2 environment making oxy steam combustion a potential advancement to oxyfuel combustion.

1. Introduction

Coal is one of the largest sources of energy in developing countries like India [1,2]. With increasing urbanization and industrialization, the demand for coal is projected to increase further. However, coal combustion for power generation is also a major source of greenhouse gas emissions [3]. The excessive emission of greenhouse gases like CO_2 has been linked with serious damage to the environment, like global warming, melting of ice caps, rise in sea levels, changes in weather patterns, and extinction of many species of flora and fauna [4]. Though renewable sources of energy like photovoltaic solar, solar thermal, hydropower, wind, etc., are effective in reducing greenhouse gas emissions, challenges such as intermittency in the supply of power, cost of setup, and requirement of space have impeded the replacement of coal-based thermal power plants [5]. Therefore, thermal power plants based on coal combustion are predicted to remain a major source of power in the energy mix of developing countries in the near future [1]. This makes the adoption of carbon capture, utilization, and storage (CCUS) imperative for mitigating the greenhouse footprint of coal power.

CCUS pertains to technologies that capture CO_2 at the source for industrial use or for sequestration in oil and gas reservoirs or saline aquifers [6]. Oxyfuel combustion is a major carbon capture technology in which the fuel undergoes combustion in a mixture of pure O_2 and recirculated flue gas composed of CO_2 or H_2O or both instead of air so that CO_2 gas with the required purity could be collected at the exhaust for utilization by industries or sequestration [7,8]. Besides carbon capture, oxyfuel combustion offers major advantages over traditional air-based power plants, such as lower NOx and SO_2 emissions, lower flue gas flow rate, and smaller flue gas treatment equipment. Based on reactor type, oxyfuel combustion of coal is classified into oxyfuel pulverized coal combustion and oxyfuel fluidized combustion [9]. Oxyfuel pulverized coal combustion involves burning of micron-sized coal particles in an oxyfuel environment at high flame temperatures which helps achieve high combustion efficiency and power density [10]. However, oxyfuel pulverized coal combustion is less suitable for high-ash

* Corresponding author.
E-mail address: david.pallares@chalmers.se (D. Pallarès).

https://doi.org/10.1016/j.fuproc.2026.108415
Received 4 December 2025; Received in revised form 14 January 2026; Accepted 2 February 2026
Available online 12 February 2026

fuels, as their reduced fixed-carbon fraction lowers overall combustibility and hinders complete burnout [10]. In contrast, oxyfuel fluidized bed combustion can effectively utilize high-ash fuels by facilitating their conversion within a bed of inert solids fluidized under oxyfuel conditions [11]. Similar to oxyfuel pulverized coal systems, it enables the conversion of existing air-fired boilers to oxyfuel operation with relatively small modifications [8]. However, for such a transformation, knowledge about the combustion characteristics of the fuel becomes essential.

Several researchers have studied the oxyfuel combustion characteristics of coal char in a fluidized bed. Investigations conducted on the effect of O_2 concentration show that the peak temperature of a char particle increases and the burnout time reduces with an increase in O_2 concentration [12–15]. In oxyfuel combustion, CO_2 and H_2O are known to react with char through gasification reactions [16]. Bu et al. [12] compared the combustion characteristics of char from coal and biomass in an O_2/N_2 and an O_2/CO_2 environment at a fluidized bed temperature of 1088 K and found the burnout time to be longer in the O_2/CO_2 environment. This was attributed to the lower diffusivity of O_2 in CO_2 when compared with N_2 [17,18]. Similar observations were made by Bhunia et al. [14], who performed high ash coal char combustion experiments in a tubular reactor in O_2/N_2 and O_2/CO_2 environment and Roy et al. [19], who performed fluidized bed experiments at a bed temperature of approximately 1173 K. Scala et al. [20,21] conducted fluidized bed experiments in different O_2 concentrations and bed temperatures and observed that at higher bed temperatures and lower O_2 concentrations, the CO_2 gasification reaction also participated in carbon conversion. However, Bu et al. [22], Saucedo et al. [23] and Salinero et al. [13] observed that the CO_2 gasification reaction could be significant even at bed temperatures less than 1173 K. Saucedo et al. [23] found that intraparticle limitations in the mass transfer of CO_2 need to be considered due to faster gasification rates in oxyfuel atmospheres at temperatures above 1173 K.

In oxyfuel fluidized bed boilers, water vapour is generated from fuel moisture and the combustion of volatiles, which can influence char combustion in the furnace by adding one more reactive agent. This effect becomes even more significant in oxyfuel systems employing wet flue gas recirculation. However, studies on oxyfuel fluidized bed combustion in the presence of water vapour have been relatively uncommon, yielding varied results among researchers. Roy et al. [19] found that the addition of steam to an O_2/CO_2 environment raised the char particle temperature and increased the carbon consumption rate. This was attributed to the water gas shift reaction of CO with H_2O. Bu et al. [22] studied the combustion of a high ash coal char particle in a fluidized bed with different concentrations of CO_2 and H_2O and observed that the burnout time is longer and peak temperature is lower in an $O_2/CO_2/H_2O$ environment when compared with the O_2/CO_2 environment, which was attributed to the endothermic H_2O gasification reaction, and competition between O_2, CO_2 and H_2O for active carbon sites. The high-ash char particles were observed to preserve their spherical shape and size throughout the experiment, as the formation of an ash skeleton inhibited particle attrition under the fluidized bed's abrasive conditions. Seepana et al. [24] proposed oxysteam combustion, where char undergoes combustion in oxygen mixed with steam, as a viable advancement to oxyfuel combustion. Li et al. [25] conducted studies on oxysteam combustion and observed that the competitive effect of H_2O significantly increased with bed temperature. However, despite competition between O_2 and H_2O in oxy steam combustion, Li et al. [15] report that O_2/H_2O combustion is better for operation under high oxygen concentration and high bed temperature due to significant enhancement in oxidation and gasification, which not only results in higher carbon conversion rates, but also ensures a relatively low particle temperature, which is beneficial in reducing pollutant emissions and reducing bed agglomeration. Although this process has many advantages, it is uncertain how to recover the energy invested in the evaporation of the water needed to replace nitrogen, which warrants future investigation. Nevertheless, the H_2O concentration is an interesting parameter and is therefore included as a parameter in the present study.

Most studies on char combustion characteristics have focused on the individual main effects of one or two significant parameters. However, a comprehensive study considering the interaction effect between several parameters, such as in this work with gas environment, particle size, and bed temperature has not been reported in literature, especially for high ash coal char. In the current study, experiments have been conducted on a batch of in situ prepared high ash coal char to measure the effects and interplays of significant parameters. In-situ prepared char ensures that the influence of thermal annealing is minimal. The application of a fast Universal Exhaust Gas Oxygen (UEGO) sensor reduces the uncertainty in O_2 concentration measurement in H_2O rich environments.

2. Experimental setup and materials

2.1. Experimental setup

The experimental setup for fluidized bed combustion studies of a batch of char particles is shown in Fig. 1(a). The schematic of the same is shown in Fig. 1(b). The experimental setup consisted of an electrically heated (6 kW) reactor section of diameter 7 cm filled with quartz sand (300–500 μm, density = 2600 kg/m^3), forming a bed of unexpanded height 5 cm. A 6-mm diameter K-type thermocouple immersed in the bed was used to sample bed temperature feedback to maintain the bed at the desired temperature. To fluidize the bed, a mass flow rate of 10 standard litres per minute (SLPM) of the desired gas mixture was supplied through a perforated plate (hole size: 500 μm) at the bottom of the reactor section, yielding superficial fluidization velocities within the range 0.156–0.185 m/s for the conditions investigated in this study. This corresponds to a fluidization number within 1.65 and 1.95 (the minimum fluidization velocity was experimentally determined to be around 0.09 m/s). The desired gas composition in the reactor section was achieved by using mass flow controllers (MFCs) to regulate the flow of O_2,CO_2 and N_2 while a steam generator controlled the flow of H_2O. The steam generator was kept at a temperature of 823 K. The flow of H_2O to the steam generator was controlled such that the sudden expansion to steam did not propagate upstream of the water flow. A wideband O_2 UEGO sensor (Bosch LSU 4.9) placed at the header section of the fluidized bed setup was used to track the O_2 concentration in the exhaust. This was used to calculate the reaction rate of char. A basket system was used to prepare in situ coal char for the experiments. The header section was enclosed with a quartz plate to allow visualization of the bed surface using a Charge Coupled Device (CCD) camera through a mirror system. The camera was fitted with an image doubler with red (610 nm) and yellow (580 nm) filters to measure char particle temperature using two-colour pyrometry.

2.2. Fuel and preparation of the char

Bituminous coal from Mahanadi coal fields in India was selected for the investigation [26]. The coal delivered from this coal field has high ash content, typical for many coals from India [27]. The proximate, ultimate and ash analysis is shown in Tables 1 and 2. The proximate analysis points at the high ash content of the coal while the ash analysis shows the different metals present in the ash. Several studies have shown that char preparation methods could have an important effect on the reaction rate of char [28,29]. To obtain a realistic estimate of the reactivity of char, the char was prepared in situ because it is known that cooled char could be affected by thermal annealing [28]. Raw coal was sieved into two different sizes: 1–1.4 mm and 2.8–3.35 mm. Sieving was achieved by placing crushed raw coal sample on the top sieve of a sieve stack which was shaked using a sieve shaker for 30 min. The sieves in the sieve stack were arranged in descending order of

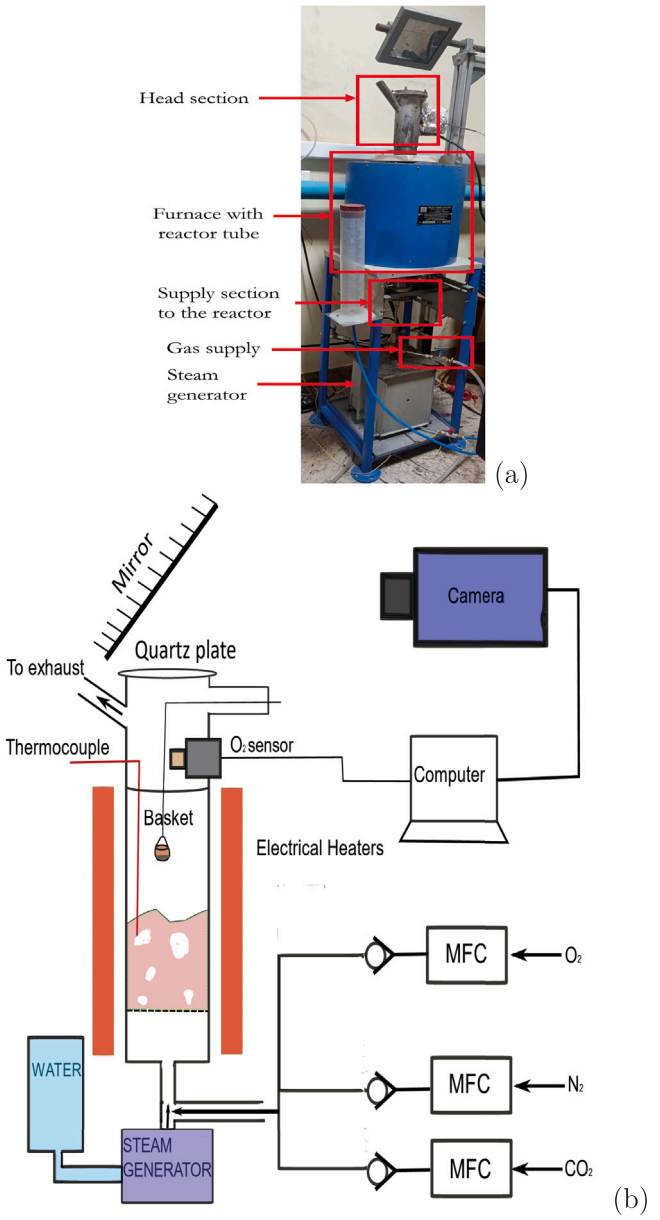

Fig. 1. Fluidized bed combustion (a) Experimental setup (b) Schematic.

mesh size, with the largest sieve at the top, and the receiver pan at the bottom. The 1–1.4 mm and 2.8–3.35 mm sized coal particles were collected from the 1 mm sieve (below the 1.4 mm sieve) and 2.8 mm sieve (below the 3.35 mm sieve) respectively. A batch of coal weighing 0.5 g was selected from the desired size and fed into an empty steel basket. The basket was attached to a steel wire, which could be used to introduce the basket into the reactor section and draw it back when required. Above the layer of coal in the basket, 10 ml of quartz sand was filled. The reactor temperature was ramped to the desired experimental condition. N_2 gas was passed at a superficial velocity of 0.11 m/s through the reactor to create an inert atmosphere in the reactor. The basket containing the coal batch covered with quartz sand is introduced into the reactor and allowed to heat up and release volatiles for 10 min, as shown in Fig. 2.

After 10 min, the basket is pulled up to the header section, and the N_2 flow is replaced with the flow used to achieve the required gas composition in the reactor. The thermal mass of the quartz sand in the basket prevents the cooling of char. It also helps reduce any char conversion during the settling time of O_2 in the reactor section. Once the

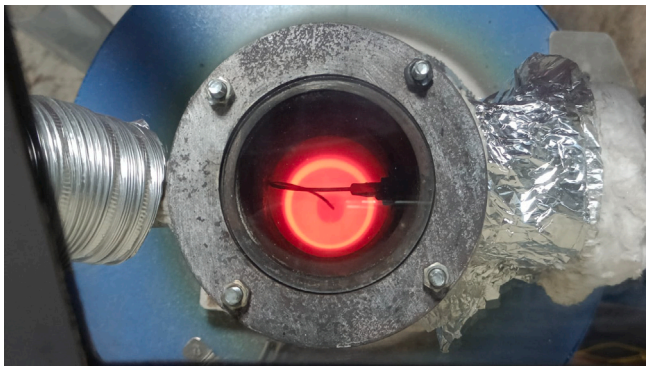

Fig. 2. Basket filled with coal particles covered with quartz sand introduced into the hot reactor environment for preparation of in-situ char.

required gas composition is achieved in the reactor, which is confirmed using the O_2 UEGO sensor, the basket is tilted, and the contents in the basket are emptied into the reactor to initiate the experiment. After emptying the basket, the basket is quickly withdrawn to allow good visualization of the bed surface. In situ prepared char helps in attaining a realistic estimate of the reactivity of char while removing ambiguity regarding any reactivity changes due to char preparation.

2.3. Reaction rate measurement

The reaction rate of char is calculated from the O_2 concentration measured at the header section of the fluidized bed setup by a Universal Exhaust Gas Oxygen (UEGO) sensor. The UEGO sensor responds to the O_2 concentration and any reactive gases such as CO and H_2 in the off-gas, from the fluidized bed [23]. Once CO and H_2 enter the cavity of the sensor, they get rapidly oxidized to CO_2 and H_2O on the platinum electrode [23,30]. This helps the UEGO sensor act as a complete combustion sensor since only one measurement is required for a full carbon balance, and O_2 measured is the residual O_2 after all reactive gases have been oxidized [23]. The reaction rate is calculated using Eq. (1):

$$Reaction\,rate, r = N_{tot}\Delta y_{oxy} M_{carbon} \tag{1}$$

where N_{tot} is the total molar flow rate (moles/(m^3s)), Δy_{oxy} is the measured change in the mole fraction of O_2 across the bed, $\Delta y_{oxy} = y_{oxy,in} - y_{oxy,measured}$ and M_{carbon} is the molar mass of carbon (kg/mol). Fig. 3 shows the reaction rate profiles of char from a coal batch of median size 1.2 -mm at 1073 K in 20% O_2/80% N_2 and 20% O_2/80% CO_2.

The burnout time of the batch of char was measured by calculating the time taken for 99% conversion to take place. The degree of conversion, X, was calculated using Eq. (2).

$$X = \frac{\int_0^{t_{burnout}} r dt}{m_{char}} \tag{2}$$

where r is the reaction rate from Eq. (1), m_{char} is the initial mass of char and $t_{burnout}$ is the burnout time.

2.4. Temperature measurement

The two-colour pyrometry technique was used to measure the surface temperature of burning char particles. A CCD camera with an image doubler was used to obtain red and yellow-filtered images of the bed surface using red (Centre wavelength: 610 nm, Full Width Half Maximum (FWHM): 10 nm) and yellow (Centre wavelength: 580 nm, FWHM: 10 nm) bandpass filters. The red filter is additionally attached to a neutral-density (Optical density:2) filter. Since the two

Table 1
Proximate and ultimate analysis of coal on as received basis (in % mass) and Gross Calorific Value (GCV(kJ/kg)).

Moisture	Ash	Volatile	GCV(kJ/kg)	C	H	O	N
6.78	43.94	24.24	15 439	45.73	3.57	9.93	0.98

Table 2
Ash analysis of high ash coal (in % by mass)

SiO_2	Al_2O_3	Fe_2O_3	CaO	MgO	Na_2O	K_2O	SO_3	Cl
57.59	29.88	5.06	2.40	1.92	0.27	0.99	1.32	–

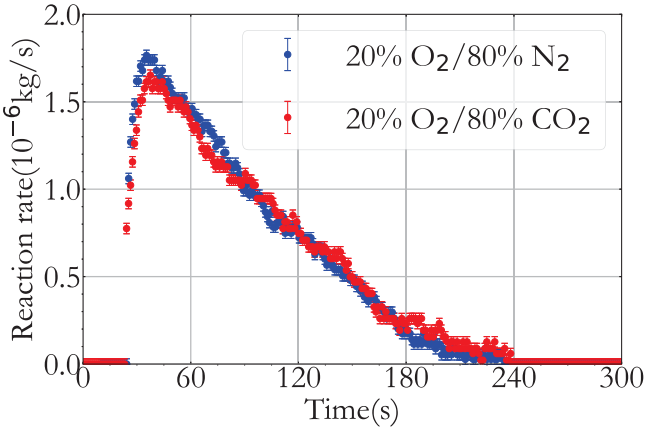

Fig. 3. Reaction Rate profile of char prepared in situ from 0.5 g batch coal of median size 3 mm at 1173 K in 20% O_2/80% N_2 and 20% O_2/80% CO_2.

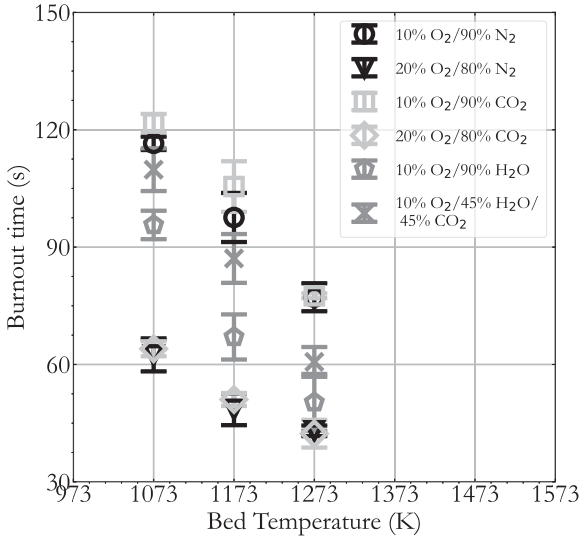

Fig. 4. Variation in burnout time of 1.2 mm sized char particles in a fluidized bed combustor.

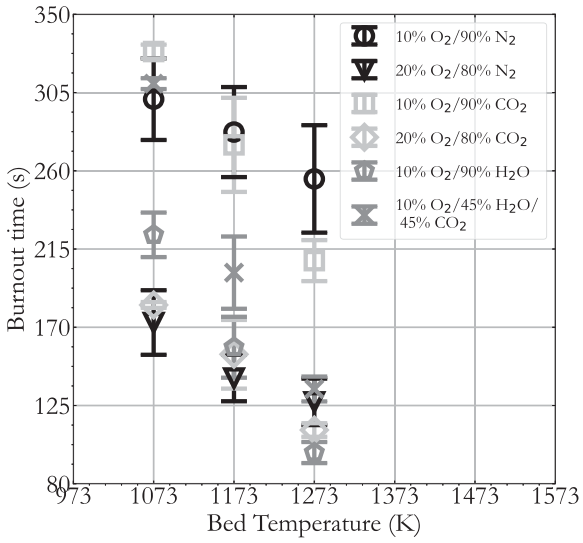

Fig. 5. Variation in burnout time of 3 mm sized char particles in a fluidized bed combustor.

wavelengths used for two colour pyrometry are very close in the electromagnetic spectrum, a grey body assumption has been made for the burning particle [31]. Similar studies have demonstrated the validity of this assumption [15,32,33]. Details regarding the calibration of the two colour pyrometer have been explained in the Supplementary material.

2.5. Experimental matrix

Table 3 shows the test matrix for fluidized bed char combustion experiments. The bed temperature varied between 1073 and 1273 K. The O_2 concentration varied between 10% and 20%. Char prepared from coal batches weighing 0.5 g and median sizes 1.2 -mm and 3 -mm were employed. The balance gas in the environment varied between CO_2, H_2O, N_2, and CO_2/H_2O in equal proportions. Every test was conducted at least three times to ensure reproducibility of the results.

3. Results and discussion

The variation in burnout time of char particles with the bed temperature for different environments is shown in Figs. 4 and 5, for 1.2 mm and 3 mm particles respectively. The difference between the median of particle surface temperature (measured when the char particle reached the surface of the fluidized bed) and bed temperature is shown in Figs. 7 and 8. The effect of char particle size, bed temperature, and gas atmosphere is discussed below. Although most studies have generally noted that the ash layer is stripped from char particle surfaces by fluidized-bed motion, observations from the present work suggest that the char particles may retain their original shape and size as an ash skeleton, despite hydrodynamic forces within the bed. This behaviour is consistent with the trends reported by Bu et al. [12,22].

3.1. Effect of bed temperature

From Figs. 4 and 5, it can be seen that increasing the bed temperature reduced the burnout time of the char for all environments and particle sizes. The extent of the reduction in burnout time was different for different environments and particle sizes, as shown in Table 4.

Table 3
Experimental matrix.

Test	Bed temperature (K)	Particle size (mm)	O_2 (vol%)	CO_2 (vol%)	H_2O (vol%)	N_2 (vol%)
1	1073	1.2	10	0	0	90
2	1073	1.2	20	0	0	80
3	1073	1.2	10	90	0	0
4	1073	1.2	20	80	0	0
5	1073	1.2	10	0	90	0
6	1073	1.2	10	45	45	0
7	1073	3	10	0	0	90
8	1073	3	20	0	0	80
9	1073	3	10	90	0	0
10	1073	3	20	80	0	0
11	1073	3	10	0	90	0
12	1073	3	10	45	45	0
13	1173	1.2	10	0	0	90
14	1173	1.2	20	0	0	80
15	1173	1.2	10	90	0	0
16	1173	1.2	20	80	0	0
17	1173	1.2	10	0	90	0
18	1173	1.2	10	45	45	0
19	1173	3	10	0	0	90
20	1173	3	20	0	0	80
21	1173	3	10	90	0	0
22	1173	3	20	80	0	0
23	1173	3	10	0	90	0
24	1173	3	10	45	45	0
25	1273	1.2	10	0	0	90
26	1273	1.2	20	0	0	80
27	1273	1.2	10	90	0	0
28	1273	1.2	20	80	0	0
29	1273	1.2	10	0	90	0
30	1273	1.2	10	45	45	0
31	1273	3	10	0	0	90
32	1273	3	20	0	0	80
33	1273	3	10	90	0	0
34	1273	3	20	80	0	0
35	1273	3	10	0	90	0
36	1273	3	10	45	45	0

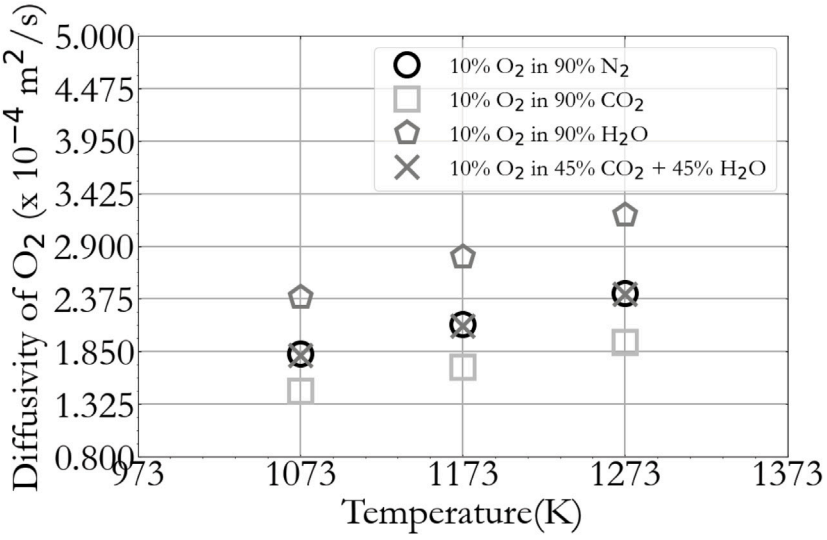

Fig. 6. Change in diffusivity of O_2 with temperature in different environments (determined from CANTERA [34])

It can be seen that the burnout time of char particles had higher sensitivity towards change in bed temperature in O_2/CO_2, O_2/H_2O and $O_2/CO_2/H_2O$ environment than in the O_2/N_2 environment. This could be attributed to the contributions from CO_2 (Reaction (3) E_a : 210–280 kJ mol^{-1} [35]) and H_2O (Reaction (4) E_a: 150–250 kJ mol^{-1} [35]) gasification reactions, which have higher activation energies than that of O_2-driven char oxidation(E_a: 130–210 kJ mol^{-1} [35]) and thus will gain relative significance with temperature.

$$C(s) + CO_2(g) \rightarrow 2CO(g) \quad \Delta H^0_{298K} = 173 \text{ kJ mol}^{-1} \tag{3}$$

Table 4
Percentage change in burnout time with increase in bed temperature (in %/K).

Environment	Particle size: 1.2 mm	Particle size: 3 mm
10% O_2/90% N_2	−0.20	−0.08
10% O_2/90% CO_2	−0.21	−0.22
20% O_2/80%N_2	−0.20	−0.16
20% O_2/80% CO_2	−0.21	−0.23
10% O_2/90% H_2O	−0.34	−0.40
10% O_2/45% CO_2/45% H_2O	−0.28	−0.44

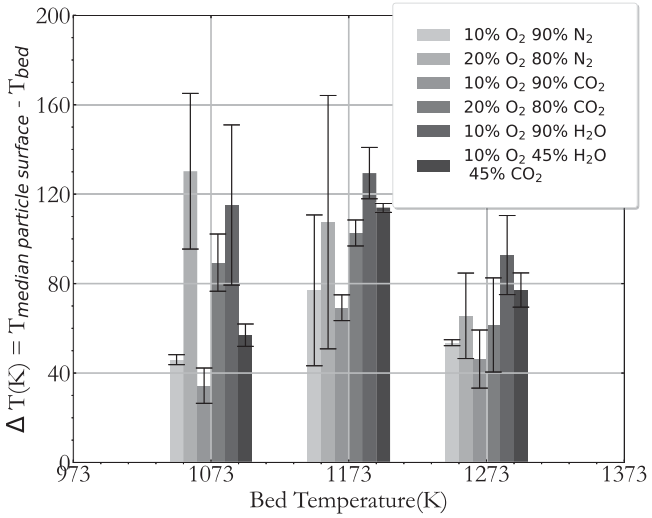

Fig. 7. Difference between the median of particle surface temperature and the bed temperature for 1.2 mm sized char particles in a fluidized bed combustor.

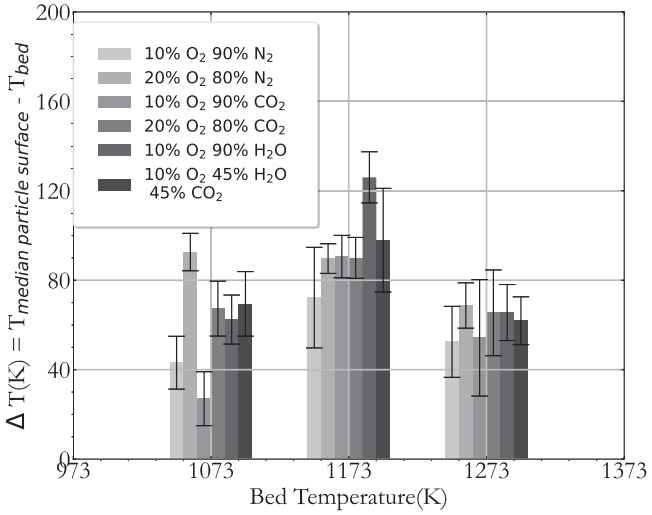

Fig. 8. Difference between the median of particle surface temperature and the bed temperature for 3 mm sized char particles in a fluidized bed combustor.

$$C(s) + H_2O(g) \rightarrow CO(g) + H_2(g) \quad \Delta H^0_{298K} = 132.5 \text{ kJ mol}^{-1} \tag{4}$$

However, it is not the case in O_2/N_2 environment where the Char-O_2 reaction is almost completely dominant and reduction in burnout time with bed temperature could be attributed to an increase in the diffusivity of O_2 (Fig. 6) and combustion kinetics with temperature.

Figs. 7 and 8 show that the median surface temperature of the char particles increased with bed temperature. This observation was intuitive since the particle temperature increases with the temperature of the combustion environment, and therefore combustion occurs at a particle temperature that follows the trend of the fluidized bed temperature. However, it is also observed that the bed temperature was the most important parameter governing the median temperature of the char particle since the difference between the bed temperature and the median particle temperature, i.e., the excess temperature of the char surface, did not exhibit any significant trend with bed temperature.

3.2. Effect of O_2 concentration

The O_2 concentration was varied between 10% and 20% in O_2/N_2 and O_2/CO_2 environments (Figs. 4 and 5). Increasing the O_2 concentration decreased the burnout time. This was mainly due to the enhancement in the mass transfer of O_2 to the char surface and its diffusivity through the ash layer [36]. Increasing the O_2 concentration yields a higher drop in burnout time than an increase in bed temperature, indicating a lower contribution from increased oxidation kinetics. However, at 10% O_2 concentration, the relative drop in burnout time with bed temperature was less drastic than at 20% O_2 concentration as seen from Table 4. This shows that the enhancement in reaction rate on increasing the bed temperature was higher in a 20% O_2 environment when compared with a 10% O_2 environment. This could be further understood from the Arrhenius oxidation model shown in reaction (5).

$$R_{v,O_2,comb} = C_{O_2} A_{O_2} exp\left(-\frac{E_{O_2}}{R_g T}\right) \tag{5}$$

where C_{O_2} is the O_2 concentration, A_{O_2} is the pre-exponential factor, E_{O_2} is the activation energy, R_g is the universal gas constant and T is the temperature. As seen from reaction (5), a higher O_2 concentration amplifies the exponential changes due to combustion at higher bed temperatures. This could be due to the higher reaction rates at higher O_2 concentrations, which contributed towards an increase in particle temperature apart from the contributions from an increase in bed temperature. For 1.2 mm particles, the drop in relative burnout time was comparable in all environments because 1.2 mm char particles undergo conversion in the kinetically controlled regime where the mass transfer of O_2 is fast relative to reaction rate kinetics [35]. Therefore, a higher O_2 concentration did not demonstrate a higher drop in relative burnout time with an increase in bed temperature. In contrast, the drop in relative burnout time was higher for 3 mm particles with an increase in O_2 concentration in an O_2/N_2 environment because 3 mm particles undergo conversion under O_2 mass transfer control [35]. In the O_2/CO_2 environment, for an increasing bed temperature, CO_2 gasification throughout the volume of the char particle [12] reduced the relative impact of temperature increase at a higher O_2 concentration when compared with that at a lower O_2 concentration. Thus, the temperature level did not play a significant role in how much the burnout time is reduced by an increase in O_2 concentration.

The median char particle temperature was higher in a 20% O_2 environment when compared with a 10% O_2 environment (Figs. 7 and 8). However, the difference reduces with bed temperature. This was also observed by Salinero et al. [13] on fluidized bed experiments with Beechwood and sub-bituminous coal. This shows a higher influence of bed temperature on particle surface temperature than O_2 concentration. However, this could be mainly due to the movement of the reaction front to the core of the particle, which results in an inert ash layer at the surface. The ash layer conducts heat to the bed from the reaction front in the particle. The presence of inert material on the surface of

Table 5
Enhancement in carbon conversion due to CO_2 and H_2O for 1.2 mm particles.

Temperature (K)	$t_{burnout,O_2/CO_2/H_2O}$(s)	$t_{burnout,O_2/N_2}$(s)	γ
1073	109.8	116.5	1.06
1173	87.1	97.6	1.12
1273	60.7	77.2	1.27

Table 6
Enhancement in carbon conversion due to CO_2 and H_2O for 3 mm particles.

Temperature (K)	$t_{burnout,O_2/CO_2/H_2O}$(s)	$t_{burnout,O_2/N_2}$(s)	γ
1073	310.1	301	0.97
1173	201.4	282	1.4
1273	134.5	255	1.9

converting char particles is confirmed when particles are found not to change their shape after combustion and leave an ash skeleton. This was also observed by Bu et al. [12]. The higher intra-particle thermal resistance could reduce the effect of the O_2 controlled combustion reaction front on the surface of the ash particle. This results in a higher relative influence of the bed temperature on the particle surface temperature when compared with O_2 concentration.

3.3. Effect of particle size

From Figs. 4 and 5, it is clear that the burnout time for 1.2 mm-sized char particles is lower than that for 3 mm particles. Table 4 compares the percentage reduction in burnout time for particle sizes of 1.2 mm and 3 mm as the fluidized bed temperature increases. The reduction is higher for 1.2 mm-sized particles in O_2/N_2 environments when compared with 3 mm-sized particles. This could be because the combustion of 1.2 mm-sized particles is more kinetically controlled than 3 mm-sized particles [35]. However, the relative reduction in burnout time was higher for 3 mm-sized particles in all other environments. This could be due to the presence of other reactive gases like CO_2 and H_2O in the environment, which participated in gasification reactions. Since gasification reactions are volumetric due to lower mass transfer limitations on CO_2 and H_2O, a larger particle size helps in higher relative contribution from gasification reactions. Moreover, in 1.2 mm particles, there could be higher competition between O_2 and other reactive gases like CO_2 and H_2O for active carbon sites in char since the conversion process is more kinetically controlled and volumetric [22]. This is unlike what happens in 3 mm particles where the conversion is more controlled by the transport of O_2 and where CO_2 and H_2O reactions are volumetric whereas O_2 reactions are at the surface of the shrinking core [35]. To further elucidate this, we define an enhancement factor, γ, which quantified the enhancement in carbon conversion rate due to the presence of CO_2 and H_2O.

$$\gamma = t_{burnout,O_2/N_2} / t_{burnout,O_2/CO_2/H_2O} \quad (6)$$

Since the diffusivity of 10% O_2 in 90% N_2 is similar to that in 45% CO_2/45% H_2O, the enhancement factor captures the effect due to reactivity of O_2, CO_2 and H_2O. Tables 5 and 6 list the values for the enhancement factor γ. Though the value of γ increased with bed temperature for both 1.2 mm and 3 mm particles, the degree of enhancement was much higher for 3 mm particles when compared with 1.2 mm particles. This could be attributed to the competition between O_2, CO_2 and H_2O in 1.2 mm particles where O_2, CO_2 and H_2O competed for the same active sites within the volume of the particle.

The variance in relative drop in burnout time with an increase in bed temperature was higher for 3 mm particles than 1.2 mm particles. This shows a higher sensitivity of 3 mm particles towards changes in the environment like O_2 concentration and balance gases. This is because the conversion of 3 mm particles is more O_2 mass transfer controlled and has a higher contribution towards conversion from char gasification reactions.

The median particle temperature was found to be higher for 1.2 mm particles than 3 mm particles on comparing Figs. 7 and 8. This is in agreement with the observations made in [26] where 6-mm particles underwent combustion at a higher particle temperature when compared with 9-mm particles. However, the difference in temperature was not found to be very high due to the formation of an inert ash layer at the surface and the influence of the fluidized bed in cooling the surface with a high heat transfer coefficient [37].

3.4. Effect of environment

As seen from Table 3, char combustion in fluidized beds was studied in 6 different environments, namely, 10% O_2/90% CO_2, 20% O_2/80% CO_2, 10% O_2/90% N_2, 20% O_2/80% N_2,10% O_2/90% H_2O and 10% O_2/45% CO_2/ 45% H_2O. From Figs. 4 and 5 and Table 4, we see that the combustion environment could have a significant effect on the burnout time and on the drop in burnout time of char particles with an increase in bed temperature. Comparing 10% O_2/90% N_2 with 10% O_2/90% CO_2 in Figs. 4 and 5, it is observed that burnout time is lower in 10% O_2/90% N_2 at 1073 K for both 1.2 mm and 3 mm particles. However, the opposite is observed at a higher temperature where the burnout time in 10% O_2/90% CO_2 becomes lower than that in 10% O_2/90% N_2. This can also be observed for 20% O_2/80% N_2 and 20% O_2/80% CO_2. From this, it is evident that substituting N_2 with CO_2 results in longer burnout times at low temperatures and shorter burnout times at higher temperatures. The lower burnout time at 1073 K is due to the lower diffusivity of O_2 in CO_2 when compared with N_2 (Fig. 6). As the bed temperature is increased, CO_2 gasification reactions (Reaction (3)) also become prominent and help in reducing the burnout time drastically, especially for 3 mm particles at 1273 K. This was also observed by Salinero et al. [13] and Bu et al. [17,22]. The contributions from CO_2 gasification reaction increased with an increase in bed temperature.

In Figs. 4 and 5, it can be seen that for 10% O_2 concentration, the burnout time was the lowest in O_2/H_2O environment followed by $O_2/CO_2/H_2O$. This could be due to the higher diffusivity of O_2 in H_2O when compared with CO_2 and N_2 and due to the faster gasification of char with H_2O (Eq. (4)). From Fig. 6, we see that the diffusivity of O_2 in 90% N_2 and in 45% CO_2/45% H_2O mixture is comparable. Hence, it can be concluded that the lower burnout time in $O_2/CO_2/H_2O$ mixture when compared to O_2/N_2 is due to the CO_2 and H_2O gasification reactions. In Fig. 5, an interesting observation is that the burnout time of 3 mm particles in 10% O_2/90% H_2O environment becomes comparable to the burnout time in 20% O_2/80% N_2 environment above 1173 K. This supports oxy-steam combustion as a candidate to convert existing air-fired power plants to oxy-steam power plants.

From Table 4, we see that the reduction in burnout time with an increase in bed temperature was the highest in a 10%O_2/90%H_2O environment for 1.2 mm particles whereas it was the highest in a 10% O_2/45% CO_2/45% H_2O environment for 3 mm particles. This depicts an enhancement in reaction rate on steam addition to the environment, which could be primarily due to the enhancement in diffusivity of

O_2 in H_2O and the increase in diffusivity with bed temperature, as seen in Fig. 6. The CO_2 gasification reaction also starts becoming more prominent above 1173 K, which enhances the reaction rate in $O_2/CO_2/H_2O$ environment. However, the relative burnout time reduction with bed temperature is highest in O_2/H_2O environment when compared with $O_2/CO_2/H_2O$ for 1.2 mm particles environment because of the competition between O_2, CO_2 and H_2O for carbon active sites throughout the volume of the particle unlike the case for 3 mm particles where conversion is O_2 mass transfer controlled and O_2 reacts in a thin reaction front while CO_2 and H_2O reactions are volume-wide.

From Figs. 7 and 8, we see that the median particle temperature is high in the 10% O_2/90% H_2O and the 10% O_2/45% CO_2/45% H_2O environment. This could be due to gaseous oxidation reactions of CO and H_2 at the surface, which gets enhanced in the presence of H_2O since the major pathway for CO oxidation is through $CO + OH \rightarrow CO_2 + H$ where OH comes from steam [38]. This was also observed by Roy and Bhattacharya [19] and Marek et al. [39], who found that char particles burnt at a higher temperature with the introduction of steam.

4. Conclusion

Oxyfuel fluidized bed combustion experiments were conducted on in-situ prepared high-ash Indian coal char prepared from coal particles of size 1.2 mm and 3 mm sieved median size in O_2/N_2, O_2/CO_2, $O_2/CO_2/H_2O$, and O_2/H_2O environments. The reaction rate of char was calculated from exhaust gas O_2 concentrations measured using a UEGO sensor. The surface temperature of the char particles was calculated using the two-colour pyrometry technique. The effect of bed temperature, O_2 concentration, particle size, and environment is studied.

The char particles were found to retain their shape and size throughout combustion due to high ash content. The effect of the oxyfuel atmosphere was found to be prominent at higher bed temperatures, lower O_2 concentrations, and larger particle sizes. For the same O_2 concentration, the burnout time was the lowest in the O_2/H_2O environment. Burnout time in low O_2 steam rich environment resembled burnout in conventional air firing at elevated temperatures. This positions oxy steam combustion as a potential advancement to conventional oxyfuel combustion. Particles of size 3 mm were found to be more sensitive to changes in the environment when compared with 1.2 mm particles. The sensitivity of 3 mm particle towards bed temperature was found to be the highest in an $O_2/CO_2/H_2O$ environment, and that for 1.2 mm particles was found in an O_2/H_2O environment. $O_2/CO_2/H_2O$ environment mimicked the diffusivity of O_2 in O_2/N_2 environment while contributing towards char conversion through gasification reactions. The char particle surface temperature was the highest in an O_2/H_2O environment and $O_2/CO_2/H_2O$ environment. Median particle surface temperature was largely determined by bed temperature. The findings reported in this work provide critical insights into the combustion behaviour of coal char in different oxyfuel environments under varied thermophysical conditions which can be useful in the design of oxyfuel boilers. These findings motivate further studies in circulating fluidized beds and at higher O_2 concentrations to assess the broader applicability of the observed behaviour.

CRediT authorship contribution statement

Sachin K.S.: Writing – review & editing, Writing – original draft, Visualization, Validation, Resources, Project administration, Methodology, Investigation, Formal analysis, Data curation, Conceptualization. **David Pallarès:** Writing – review & editing, Supervision, Investigation, Formal analysis, Conceptualization. **Bo Leckner:** Writing – review & editing, Supervision, Investigation, Formal analysis, Conceptualization. **Pratikash Panda:** Writing – review & editing, Supervision, Project administration, Funding acquisition, Formal analysis, Conceptualization. **R.V. Ravikrishna:** Writing – review & editing, Supervision, Project administration, Funding acquisition, Formal analysis, Conceptualization.

Declaration of competing interest

We have no conflicts of interest to disclose.

Acknowledgements

The authors acknowledge the financial support provided by DST, India through sanction order no. TMD/CERI/CleanCoal/2017/034. The author Sachin K S thanks the support from the Prime Minister's Research Fellowship scheme of the Ministry of Education, Government of India.

Appendix A. Supplementary data

Supplementary material related to this article can be found online at https://doi.org/10.1016/j.fuproc.2026.108415.

Data availability

Data will be made available on request.

References

[1] CEA Annual Report 2023-24, Central Electricity Authority, Ministry of Power, Government of India, URL https://cea.nic.in/wp-content/uploads/annual_reports/2024/Final_Approved_Annual_Report_2023_24_05032025_1.pdf.
[2] M.A. Habib, R. Khan, Environmental impacts of coal-mining and coal-fired power-plant activities in a developing country with global context, in: Spatial Modeling and Assessment of Environmental Contaminants: Risk Assessment and Remediation, Springer, 2021, pp. 421–493.
[3] H.H. Ahmad, F. Saleem, H. Arif, et al., Evaluation of catastrophic global warming due to coal combustion, Int. J. Innov. Sci. Technol. 3 (4) (2021) 198–207.
[4] D.W. Kweku, O. Bismark, A. Maxwell, K.A. Desmond, K.B. Danso, E.A. Oti-Mensah, A.T. Quachie, B.B. Adormaa, Greenhouse effect: greenhouse gases and their impact on global warming, J. Sci. Res. Rep. 17 (6) (2018) 1–9.
[5] S.R. Sinsel, R.L. Riemke, V.H. Hoffmann, Challenges and solution technologies for the integration of variable renewable energy sources—a review, Renew. Energy 145 (2020) 2271–2285.
[6] J. Gibbins, H. Chalmers, Carbon capture and storage, Energy Policy 36 (12) (2008) 4317–4322.
[7] R. Stanger, T. Wall, R. Spörl, M. Paneru, S. Grathwohl, M. Weidmann, G. Scheffknecht, D. McDonald, K. Myöhänen, J. Ritvanen, et al., Oxyfuel combustion for CO_2 capture in power plants, Int. J. Greenh. Gas Control. 40 (2015) 55–125.
[8] B. Leckner, A. Gómez-Barea, Oxy-fuel combustion in circulating fluidized bed boilers, Appl. Energy 125 (2014) 308–318.
[9] C. Bu, A. Gómez-Barea, B. Leckner, X. Chen, D. Pallarès, D. Liu, P. Lu, Oxy-fuel conversion of sub-bituminous coal particles in fluidized bed and pulverized combustors, Proc. Combust. Inst. 36 (3) (2017) 3331–3339.
[10] L. Chen, S.Z. Yong, A.F. Ghoniem, Oxy-fuel combustion of pulverized coal: Characterization, fundamentals, stabilization and CFD modeling, Prog. Energy Combust. Sci. 38 (2) (2012) 156–214.
[11] H. Mathekga, B. Oboirien, B.C. North, A review of oxy-fuel combustion in fluidized bed reactors, Int. J. Energy Res. 40 (7) (2016) 878–902.
[12] C. Bu, D. Pallarès, X. Chen, A. Gómez-Barea, D. Liu, B. Leckner, P. Lu, Oxy-fuel combustion of a single fuel particle in a fluidized bed: Char combustion characteristics, an experimental study, Chem. Eng. J. 287 (2016) 649–656.
[13] J. Salinero, A. Gómez-Barea, D. Fuentes-Cano, B. Leckner, The influence of CO_2 gas concentration on the char temperature and conversion during oxy-fuel combustion in a fluidized bed, Appl. Energy 215 (2018) 116–130.
[14] S. Bhunia, A.K. Sadhukhan, P. Gupta, Modelling and experimental studies on oxy-fuel combustion of coarse size coal char, Fuel Process. Technol. 158 (2017) 73–84.
[15] L. Li, L. Duan, Z. Yang, S. Tong, E.J. Anthony, C. Zhao, Experimental study of a single char particle combustion characteristics in a fluidized bed under O_2/H_2O condition, Chem. Eng. J. 382 (2020) 122942.
[16] L. Li, S. Tong, L. Duan, C. Zhao, Z. Shi, Effect of CO_2 and H_2O on lignite char structure and reactivity in a fluidized bed reactor, Fuel Process. Technol. 211 (2021) 106564.
[17] C. Bu, A. Gómez-Barea, X. Chen, B. Leckner, D. Liu, D. Pallarès, P. Lu, Effect of CO_2 on oxy-fuel combustion of coal-char particles in a fluidized bed: Modeling and comparison with the conventional mode of combustion, Appl. Energy 177 (2016) 247–259.
[18] I. Guedea, D. Pallarès, L.I. Díez, F. Johnsson, Conversion of large coal particles under O2/N2 and O2/CO2 atmospheres—Experiments and modeling, Fuel Process. Technol. 112 (2013) 118–128.

[19] B. Roy, S. Bhattacharya, Combustion of single char particles from victorian brown coal under oxy-fuel fluidized bed conditions, Fuel 165 (2016) 477–483.
[20] F. Scala, R. Chirone, Combustion of single coal char particles under fluidized bed oxyfiring conditions, Ind. Eng. Chem. Res. 49 (21) (2010) 11029–11036.
[21] F. Scala, R. Chirone, Fluidized bed combustion of single coal char particles at high CO_2 concentration, Chem. Eng. J. 165 (3) (2010) 902–906.
[22] C. Bu, A. Gómez-Barea, B. Leckner, X. Wang, J. Zhang, G. Piao, The effect of H_2O on the oxy-fuel combustion of a bituminous coal char particle in a fluidized bed: experiment and modeling, Combust. Flame 218 (2020) 42–56.
[23] M.A. Saucedo, M. Butel, S.A. Scott, N. Collings, J.S. Dennis, Significance of gasification during oxy-fuel combustion of a lignite char in a fluidised bed using a fast UEGO sensor, Fuel 144 (2015) 423–438.
[24] S. Seepana, S. Jayanti, Steam-moderated oxy-fuel combustion, Energy Convers. Manage. 51 (10) (2010) 1981–1988.
[25] L. Li, L. Duan, S. Tong, E.J. Anthony, Combustion characteristics of lignite char in a fluidized bed under O_2/N_2, O_2/CO_2 and O_2/H_2O atmospheres, Fuel Process. Technol. 186 (2019) 8–17.
[26] K. Sachin, P. Panda, R. Ravikrishna, Study on the combustion of a high ash single coal particle on a flat flame burner simulating the thermal and chemical environment in a oxyfuel fluidized bed, in: International Heat Transfer Conference Digital Library, Begel House Inc. 2023.
[27] R. Singh, S. Sinha, Beneficiation of high ash Indian coal-problems and prospects, Indian Min. Eng. J. (2003) 1–4.
[28] Z. Li, R. Zou, Y. Xu, Y. Fang, G. Luo, H. Yao, Characterization of in-situ and cooling char from ten typical Chinese coals, Combust. Flame 238 (2022) 111884.
[29] C. Chen, J. Wang, W. Liu, S. Zhang, J. Yin, G. Luo, H. Yao, Effect of pyrolysis conditions on the char gasification with mixtures of CO_2 and H_2O, Proc. Combust. Inst. 34 (2) (2013) 2453–2460.
[30] N. Collings, K. Hegarty, T. Ramsander, Steady-state modelling of the universal exhaust gas oxygen (UEGO) sensor, Meas. Sci. Technol. 23 (8) (2012) 085108.
[31] Y. Huang, Y. Yan, G. Riley, Vision-based measurement of temperature distribution in a 500-kW model furnace using the two-colour method, Measurement 28 (3) (2000) 175–183.
[32] O. Chansa, Z. Luo, E.G. Eddings, C. Yu, Determination of alkali release during oxyfuel co-combustion of biomass and coal using laser-induced breakdown spectroscopy, Fuel 289 (2021) 119658, http://dx.doi.org/10.1016/j.fuel.2020.119658.
[33] L. Li, L. Duan, Z. Yang, C. Zhao, Pressurized oxy-fuel combustion characteristics of single coal particle in a visualized fluidized bed combustor, Combust. Flame 211 (2020) 218–228.
[34] D.G. Goodwin, H.K. Moffat, I. Schoegl, R.L. Speth, B.W. Weber, Cantera: An object-oriented software toolkit for chemical kinetics, thermodynamics, and transport processes, 2025, http://dx.doi.org/10.5281/zenodo.17620923, Version 3.2.0, https://www.cantera.org.
[35] N.M. Laurendeau, Heterogeneous kinetics of coal char gasification and combustion, Prog. Energy Combust. Sci. 4 (4) (1978) 221–270.
[36] F. Scala, Fluidized-bed combustion of single coal char particles: An analysis of the burning rate and of the primary CO/CO_2 ratio, Energy Fuels 25 (3) (2011) 1051–1059.
[37] G. Palchonok, A. Dolidovich, S. Andersson, B. Leckner, Calculation of true heat and mass transfer coefficients between particles and a fluidized bed, in: Proc of the 7th Engineering Foundation Conference on Fluidization, vol. 7, 1992, pp. 913–920.
[38] C.K. Law, Combustion Physics, Cambridge University Press, 2010.
[39] E. Marek, B. Świątkowski, Reprint of "Experimental studies of single particle combustion in air and different oxy-fuel atmospheres", Appl. Therm. Eng. 74 (2015) 61–68.